Short Title

Title

By

Ian D. Roberts, B.Sc.

A Thesis

Submitted to the School of Graduate Studies

in Partial Fulfilment of the Requirements

for the Degree

Master of Science

McMaster University

Master of Science (2016) McMaster University

(Physics and Astronomy) Hamilton, Ontario

TITLE: Title

AUTHOR: Ian Roberts, B.Sc. (McMaster University)

SUPERVISORS: Laura Parker

NUMBER OF PAGES: viii, 21

Abstract

Abstract...

Acknowledgements

Acknowledgements here

dedication here

Table of Contents

List of Figures

List of Tables

Chapter 1

Introduction

Chapter 2

Mass segregation trends in SDSS galaxy groups

2.1 Introduction

It has been well established that galaxy properties dpend strongly on local environment (e.g. Oemler, 1974; Hogg et al., 2004; Blanton et al., 2005a; Tal et al., 2014). Galaxies in dense environments such as clusters tend to have lower star formation rates (SFRs), while isolated field galaxies are generally actively forming stars (e.g. Balogh et al., 2000; Ball et al., 2008; Wetzel et al., 2012). It is also well known that galaxy properties, such as SFR, depend strongly on galaxy mass (e.g. Poggianti et al., 2008). It is critical to study the distribution of galaxy masses within haloes of different masses in order to ascertain whether the variations in galaxy properties with environment are due to physical mechanisms acting in dense environments, or simply due to the fact that high-density environments contain more high-mass galaxies. Intermediate-density environments, galaxy groups, represent not only the most common environment in the local Universe (Geller & Huchra, 1983; Eke

et al., 2005), but also represent the environment where many physical processes are efficient. Galaxy interactions such as mergers and harassment are favoured in this environment because of the low relative velocities between galaxies (Zabludoff & Mulchaey, 1998; Brough et al., 2006).

The study of mass segregation in groups can be used to elucidate information on physical processes such as dynamical friction, galaxy mergers, and tidal stripping. Mass segregation in bound structures has generally been predicted as a result of dynamical friction (Chandrasekhar, 1943). Dynamical friction acts as a drag force on orbiting bodies and massive galaxies within groups and clusters are expected to migrate to smaller radii as time progresses. If dynamical friction is a dominant factor, then clear mass segregation should be observed in evolved groups and clusters.

Galaxy groups are not static systems, but are constantly being replenished by infalling galaxies from the field. Infalling galaxies are preferentially found at large radii (Wetzel et al., 2013) and the difference in stellar mass distributions between evolved group members and infalling galaxies could affect the strength of mass segregation.

If significant mass segregation is not found, then this implies that either: the time-scale associated with dynamical friction is greater than the age of the group/cluster, or that there are other physical processes, such as merging, tidal stripping, or pre-processing, which are playing a more important role than dynamical friction.

Recent work has shown conflicting results with regards to the presence of mass segregation in groups and clusters. Ziparo et al. (2013) find no evidence

for strong mass segregation in X-ray selected groups out to $z = 1.6$, for a sample of galaxies with $M_{\rm star} > 10^{10.3}{\rm M}_{\odot}$. von der Linden et al. (2010) examine Sloan Digital Sky Survey (SDSS) galaxy clusters and find no evidence for mass segregation in four different redshift bins at $z < 0.1$. von der Linden et al. make redshift-dependent stellar mass cuts ranging from $10^{9.6}$ to $10^{10.5}{\rm M}_{\odot}$. Vulcani et al. (2013) use mass-limited samples at $0.3 \leq z \leq 0.8$ from the IMACS Cluster Building Survey and the ESO Distant Cluster Survey, with stellar mass cuts at $M_{\rm star} > 10^{10.5}{\rm M}_{\odot}$ and $M_{\rm star} > 10^{10.2}{\rm M}_{\odot}$, respectively, to study galaxy stellar mass functions in different environments. Vulcani et al. find no statistical differences between mass functions of galaxies located at different cluster-centric distances.

Conversely, Balogh et al. (2014) find evidence for mass segregation in Group Environment Evolution Collaboration 2 (GEEC2) groups at $0.8 < z < 1$, using as stellar-mass-limited sample with $M_{\rm star} > 10^{10.3}{\rm M}_{\odot}$. Using a volume limited sample of zCOSMOS groups, Presotto et al. (2012) find evidence for mass segregation in their whole sample at both $0.2 \leq z \leq 0.45$ and $0.45 \leq z \leq 0.8$. Presotto et al. also break their sample into rich and poor groups at $0.2 \leq z \leq 0.45$, and find evidence for mass segregation within rich groups but find no evidence for mass segregation within poor groups. Using a $V_{\rm max}$-weighted sample with a stellar mass cut at $10^{9.0}{\rm M}_{\odot}$, van den Bosch et al. (2008) find evidence for mass segregation in SDSS groups.

It is clear that there is no consensus regarding the strength of mass segregation in groups and clusters or its halo mass dependence.

In this Letter, we present evidence of the presense of a small, but significant, amount of mass segregation in SDSS galaxy groups. We show that the detection of mass segregation is dependent on stellar mass completeness, with completeness cuts at relatively high stellar masses potentially masking underlying mass segregation trends. We also show that the strength of mass segregation scales inversely with halo mass, with cluster-sized haloes showing little to no observable mass segregation. In Section 2.2, we briefly describe our data set, in Section 2.3 we present our results from this work, in Section ... we provide a discussion of our results, and in Section ... we give a summary of the results and make concluding statements.

In this Letter, we assume a flat Λ cold dark matter cosmology with $\Omega_M = 0.3$, $\Omega_\Lambda = 0.7$, and $H_0 = 70\,\mathrm{km\,s^{-1}\,Mpc^{-1}}$.

2.2 Data

The results presented in this Letter utilize the group catalogue of Yang et al. (2007). This catalogue is contructed by applying the halo-based group finder of Yang et al. (2005, 2007) to the New York University Value-Added Galaxy Catalogue (NYU-VAGC; Blanton et al. 2005b), which is based on the SDSS Data Release 7 (DR7; Abazajian et al. 2009. Stellar masses are obtained from the NYU-VAGC and are computed using the methodology of Blanton & Roweis (2007), assuming a Chabrier (2003) initial mass function. Halo masses are determined using the ranking of the characteristic stellar mass, $M_{\star,\mathrm{grp}}$, and assuming a relationship between M_{halo} and $M_{\star,\mathrm{grp}}$ (Yang et al., 2007). $M_{\star,\mathrm{grp}}$ is defined by Yang et al. as

$$M_{\star,\mathrm{grp}} = \frac{1}{g(L_{19.5},\, L_{\mathrm{lim}})} \sum_i \frac{M_{\mathrm{star},i}}{C_i}, \tag{2.1}$$

where $M_{\mathrm{star},i}$ is the stellar mass of the ith member galaxy, C_i is the completeness of the survey at the position of that galaxy, and $g(L_{19.5},\, L_{\mathrm{lim}})$ is a correction factor which accounts for galaxies missed due to the magnitude limit of the survey.

Halo-centric distance for each galaxy is not given explicitly in the Yang catalogue; however, we calculate it using the redshift of the group and the angular separation of the galaxy and halo centre on the sky. We measure group-centric radius from the luminosity-weighted centre of each group, and normalize our grou-centric radii by R_{200}. We use the definition for R_{200} as given in Carlberg et al. (1997)

$$R_{200} = \frac{\sqrt{3}\sigma}{10H(z)}, \tag{2.2}$$

where the Hubble parameter, $H(z)$, is defined as

$$H(z) = H_0\sqrt{\Omega_M(1+z)^3 + \Omega_\Lambda}, \tag{2.3}$$

and we calculate the velocity dispersion, σ, as

$$\sigma = 397.9\,\mathrm{km\,s^{-1}} \left(\frac{M_{\mathrm{halo}}}{10^{14}\,h^{-1}\mathrm{M}_\odot}\right)^{0.3214}, \tag{2.4}$$

where the above is a fitting function given in Yang et al. (2007).

For our analysis we select group galaxies with redshift, $z < 0.1$, that are within two virial radii of the group centre, and groups with a minimum of three galaxy members – although our results are not sensitive to these specific cuts. For our sample over 95 per cent of group galaxies reside within two virial radii of the group centre. We also subtract the most massive galaxy (MMG) from each group, to ensure that any underlying radial mass trend is not contaminated by the MMG.

This sample is not volume limited, therefore, the sample will suffer from the Malmquist bias. This leads to a bias towards objects of higher luminosity and stellar mass, with increasing redshift. To account for this bias we weight our sample by $1/V_{\rm max}$, where $V_{\rm max}$ is the comoving volume of the Universe out to a comoving radius at which the galaxy would have met the selection criteria for the sample. For our $V_{\rm max}$ weights we apply the values presented in the catalogue of Simard et al. (2011) to our sample.

In order to investigate the effect of stellar mass limits on the detection of mass segregation, we use samples corresponding to various stellar mass cuts. We perform our analysis on an unweighted sample with two mass cuts corresponding to $M_{\rm star} > 10^{10.5}{\rm M}_{\odot}$ (4152 galaxies in 1970 groups) and $M_{\rm star} > 10^{10.0}{\rm M}_{\odot}$ (26 774 galaxies in 4534 groups); and a $V_{\rm max}$-weighted sample with mass cuts at $M_{\rm star} > 10^{9.0}{\rm M}_{\odot}$ (56 957 galaxies in 7217 groups) and $M_{\rm star} > 10^{8.5}{\rm M}_{\odot}$ (59 791 galaxies in 7289 groups). The unweighted sample is stellar mass complete down to $M_{\rm star} > 10^{10.0}{\rm M}_{\odot}$. Therefore, for both the weighted and unweighted sample, we have two different stellar mass cuts, giving us four separate samples in total.

2.3 Results

2.3.1 Mass segregation in SDSS groups

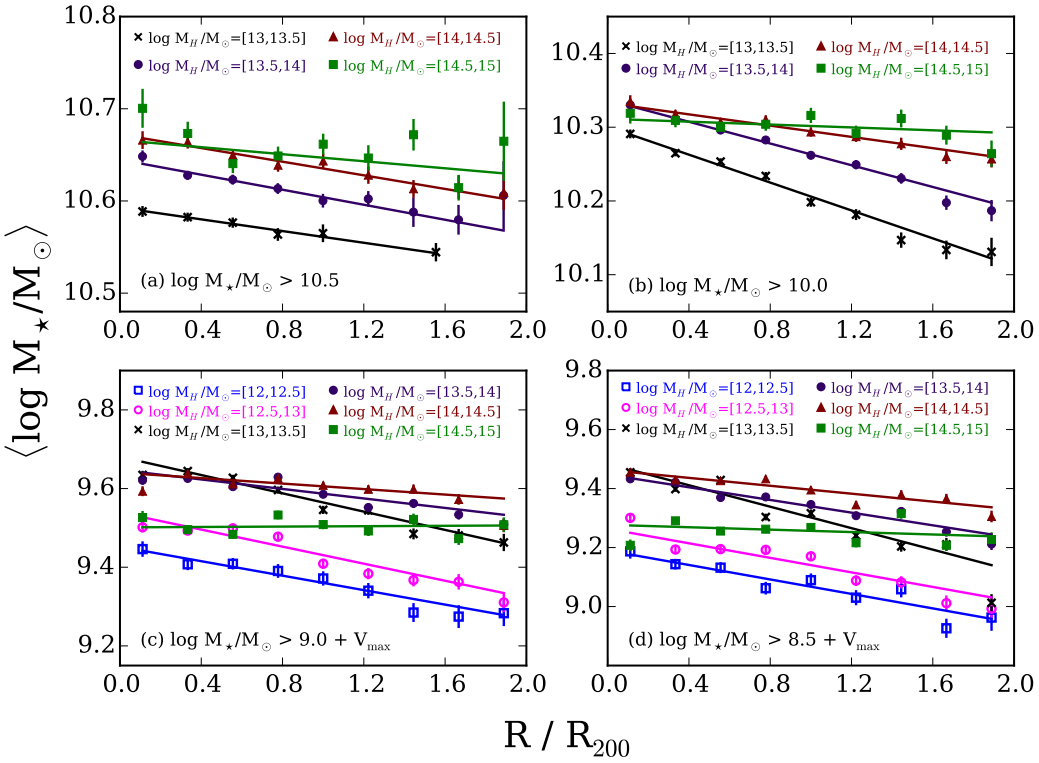

Figure 2.1 All panels show mean mass as a function of normalized distance for various halo mass bins, with error bars corresponding to 1σ statistical errors. The solid lines correspond to weighted least-squares fits for each halo mass bin. Top left: unweighted sample, for galaxies with $\log(M_{\rm star}/{\rm M}_\odot) > 10.5$. Top right: unweighted sample, for galaxies with $\log(M_{\rm star}/{\rm M}_\odot) > 10.0$. Bottom left: $V_{\rm max}$-weighted sample, for galaxies with $\log(M_{\rm star}/{\rm M}_\odot) > 9.0$. Bottom right: $V_{\rm max}$-weighted sample, for galaxies with $\log(M_{\rm star}/{\rm M}_\odot) > 8.5$. Note that different mass scales are used in each panel. There are more halo mass bins in the bottom row due to the increased number of low-mass galaxies as a result of $V_{\rm max}$ weighting.

In Fig. 2.1 we plot mean stellar mass as a function of radial distance from the group centre for various halo mass bins. Fig 2.1(a) corresponds to our

high-mass cut, unweighted sample; Fig 2.1(b) corresponds to our low-mass cut, unweighted sample; Fig 2.1(c) corresponds to our high-mass cut, weighted sample; and Fig 2.1(d) corresponds to our low-mass cut, weighted sample.

For all halo mass bins, and regardless of the mass cut, the unweighted sample shows statistically significant mass segregation with a weighted linear least-squares fit. The $V_{\rm max}$-weighted sample shows statistically significant mass segregation for the five lower halo mass bins, whereas the highest halo mass bin has a best-fitting slope consistent with zero – this trend hold for both mass cuts. For both the weighted and unweighted samples there is a clear trend of the slope with halo mass – more massive haloes show weaker mass segregation. This result will be discussed in Section ...

We find that our highest halo mass sample ($M_{\rm halo} > 10^{14.5}{\rm M}_{\odot}$) has a large number of low-mass galaxies when compared to the high-halo-mass samples, which leads to a smaller mean stellar mass in the $V_{\rm max}$-weighted results shown in Figs 2.1(c) and (d). While this introduces a shift in normalization, it does not affect the mass segregation trend and therefore does not change the key result that mass segregation depends on halo mass.

2.3.2 Massive galaxy fraction

An alternative way to investigate galaxy populations within the group sample is to study the fraction of 'massive' galaxies at various group-centric radii. In Fig..., we plot the fraction of massive galaxies as a function of radial distance for two different definitions of what constitutes a massive galaxy. We calculate the massive fraction for each radial bin as

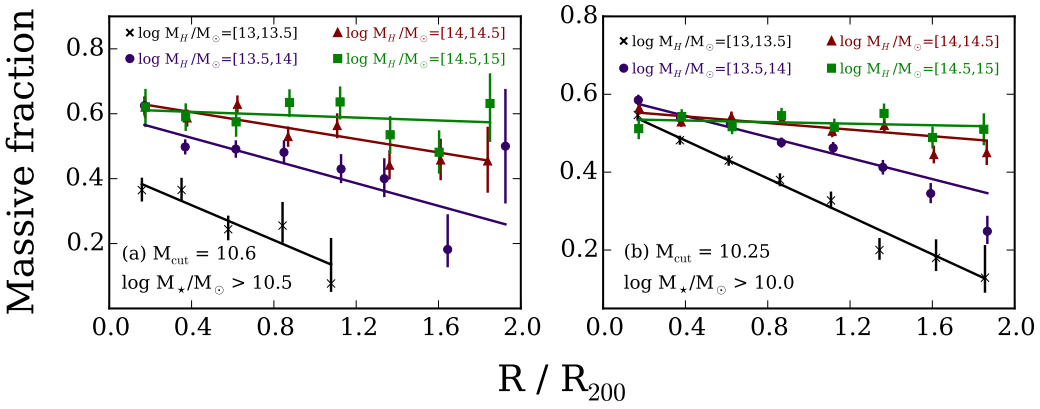

Figure 2.2 Fraction of massive galaxies with respect to normalized radial distance. Error bars are given by a 1σ binomial confidence interval, calculated using the beta distribution as outlined in Cameron (2011). The solid lines correspond to weighted least-squares fits for each halo mass bin. Left-hand panel: the fraction of galaxies with $\log(M_{\rm star}/{\rm M}_\odot) > 10.25$ as a function of radial distance, for the unweighted sample with $M_{\rm star} > 10^{10}{\rm M}_\odot$. Right-hand panel: the fraction of galaxies with $\log(M_{\rm star}/{\rm M}_\odot) > 10.5$ as a function of radial distance, for the unweighted sample with $M_{\rm star} > 10^{10}{\rm M}_\odot$.

$$f_m(M_{\rm cut}) = \frac{\#\text{ galaxies with } M_{\rm star} > M_{\rm cut}}{\#\text{ galaxies with } M_{\rm star} > 10^{10}{\rm M}_\odot}, \tag{2.5}$$

where $M_{\rm cut}$ is a stellar mass cut-off above which we define a massive galaxy. We initially apply a high-mass galaxy cut, $M_{\rm cut}$, at $10^{10.25}{\rm M}_\odot$, corresponding to the median stellar mass of the unweighted sample (with the low-mass cut at $10^{10}{\rm M}_\odot$). Comparing Figs 2.1(b) and 2.2(a) we see essentially identical trends. We observe the same trends of mass segregation whether we look at the average galaxy mass at a given radius, or consider the fraction of massive galaxies.

To confirm that this trend is robust regardless of the mass cut-off used to define a massive galaxy, we make the same plot but now use $M_{\rm cut} = 10^{10.5}{\rm M}_\odot$. Comparing Figs 2.2(a) and (b) we see that while the overall fractions of massive

galaxies decrease with increasing the stellar mass cut, the trend essentially stays the same. There is clear evidence for mass segregation and the strength of mass segregation depends on halo mass.

2.4 Discussion

2.4.1 Effect of including low-mass galaxies

The results in Fig. 2.1 show that mass segregation generally increases when lower mass galaxies are included. To quantify this effect we can compare the best-fitting slopes corresponding to the high-mass and the low-mass cut samples.

For a given halo mass, the low-mass cut sample displays larger slopes than the high-mass cut sample for two of the halo mass bins. The slopes corresponding to the other two halo mass bins are consistent with being equal. For the weighted samples we find similar results with the low-mass cut sample showing larger slopes for three of the halo mass bins, and the other three halo mass bins showing slopes consistent with being equal.

This suggests that the inclusion of low-mass galaxies has a measurable effect on the observation of mass-segregation. Studies which make mass cuts at moderate to high-stellar mass, are potentially missing a mass segregation contribution from low-mass galaxies. The observation of mild mass segregation is consistent with the low redshift sample of Ziparo et al. (2013); however, they see similar mass-radius relations regardless of the stellar mass cut applied.

2.4.2 Halo mass dependence

Figs 2.1 and 2.2 clearly indicate that the highest halo mass bins show the least mass segregation. This trend is consistent in all cases, regardless of stellar mass cut or whether the sample had $V_{\rm max}$ weights applied. Our observed dependence on halo mass is consistent with results finding no measurable mass segregation in galaxy clusters (Pracy et al., 2005; von der Linden et al., 2010; Vulcani et al., 2013)

It has been shown through N-body simulations that the dynamical friction time-scale scales with M_h/M_s (e.g. Taffoni et al., 2003; Conroy et al., 2007; Boylan-Kolchin et al., 2008), where M_s is the initial satellite mass and M_h is the mass of the host halo. For a given satellite mass, this implies a longer dynamical friction time-scale for larger haloes, which is consistent with our result. This can be interpreted as an increase in tidal stripping efficiency as M_h/M_s increases (Taffoni et al., 2003). Gan et al. (2010) have shown that for an infalling satellite the dynamical friction time-scale increases with a stronger tidal field. This is due to tidal stripping retarding the decay of satellite angular momentum, which increases the dynamical friction time-scale.

It should be noted that the merger time-scale scales with M_s/M_h Jiang et al. (2008), which implies a higher merger efficiency in low-mass haloes, for a given satellite mass. The build-up of massive objects through galaxy mergers could enhance mass segregation in low-mass haloes, in accordance with our results.

There has been evidence of cluster galaxies having their star formation quenched in lower mass groups ($\sim 10^{13}\mathrm{M}_{\odot}$) prior to accretion into the cluster

environment (e.g. Zabludoff & Mulchaey, 1998; McGee et al., 2009; De Lucia et al., 2012; Hou et al., 2014). This pre-processing could potentially provide an explanation of our observed mass segregation trends with halo mass. If mass segregation is present in the group environment as a result of pre-processing, the recent accretion of multiple pre-processed groups to form a galaxy cluster could result in little to no observed mass segregation in the cluster as a whole. In other words, if the cluster environment consists of multiple subhaloes at various cluster-centric radii, while individual subhaloes may show mass segregation, the total effect of these subhaloes together may leave the cluster with a relatively uniform radial mass distribution.

Vulcani et al. (2014) apply semi-analytic models to the Millenium Simulation (Springel et al., 2005) to study galaxy mass functions in different environments. Vulcani et al. simulate galaxy mass functions for three halo masses, $\log(M_{\rm halo}/M_{\odot}) = \{13.4, 14.1, 15.1\}$, as a function of cluster-centric radius. In the lowest mass halo they find the mass function depends slightly on cluster-centric radius, with the innermost regions showing flatter mass functions at low and intermediate masses. This trend persists, but is not as strong at intermediate halo mass. The highest halo mass bin shows virtually identical mass function shapes for all cluster-centric radii. This result is indicative of measurable mass segregation for the low- and intermediate-mass haloes, with the strength of mass segregation decreasing with increasing halo mass. These simulation trends show excellent agreement with our observed dependence of mass segregation on halo mass.

2.4.3 Reconciling previous results

In Section 2.1, we mention previous literature results which presente vidence both for and against the presence of mass segregation in groups and clusters. We argue that the majority of these results can be reconciled with our two main findings.

(i) Mass segregation is enhanced with the inclusion of low-mass galaxies in a sample.

(ii) Mass segregation decreases with increasing halo mass, with high-mass haloes showing little to no mass segregation.

Of the studies mentioned in Section 2.1, those which observe no evidence for mass segregation either: make a mass completeness cut at intermediate to high stellar mass, or observe this lack of mass segregation only in high-mass haloes. Therefore, the lack of observed mass segregation can potentially be explained through the lack of low-mass galaxies in the study survey, or the study being limited to high-halo-mass environments.

2.5 Conclusion

In this Letter, we examine mass segregation trends in the Yang et al. (2007) SDSS DR7 groups for various stellar and halo mass cuts. WE show that a small, but significant, amount of mass segregation is present in these groups. This mass segregation shows consistent trends, with lower stellar mass samples showing stronger mass segregation, and galaxies in large haloes showing little to no mass segregation.

The magnitude of mass segregation we measure, especially in high-mass haloes, is potentially indicative of dynamical friction not acting efficiently. We discuss previous literature to provide possible explanations for the observed trends, showing that our observed trends with halo mass agree with prior results. Further work with hydrodynamic simulations would be helpful to further constrain the important mechanisms responsible for our observed mass trends and the lack of mass segregation in high-mass haloes.

2.6 Acknowledgements

We thank the anonymous referee for their various helpful comments and suggestions. IDR and LCP thank the National Science and Engineering Research Council of Canada for funding. We thank X. Yang et al. for making their SDSS DR7 group catalogue public, L. Simard et al. for the publication of their SDSS DR7 morphology catalogue, and the NYU-VAGC team for the publication of their SDSS DR7 catalogue. This research would not have been possible without these public catalogues.

Funding for the SDSS has been provided by the Alfred P. Sloan Foundation, the Participating Institutions, the National Science Foundation, the US Department of Energy, the National Aeronautics and Space Administration, the Japanese Monbukagakusho, the Max Planck Society, and the Higher Education Funding Council for England. The SDSS website is http://www.sdss.org/.

Bibliography

Abazajian, K. N., Adelman-McCarthy, J. K., Agüeros, M. A., Allam, S. S., Allende Prieto, C., An, D., Anderson, K. S. J., Anderson, S. F., Annis, J., Bahcall, N. A., & et al. 2009, ApJS, 182, 543

Ball, N. M., Loveday, J., & Brunner, R. J. 2008, MNRAS, 383, 907

Balogh, M. L., McGee, S. L., Mok, A., Wilman, D. J., Finoguenov, A., Bower, R. G., Mulchaey, J. S., Parker, L. C., & Tanaka, M. 2014, MNRAS, 443, 2679

Balogh, M. L., Navarro, J. F., & Morris, S. L. 2000, ApJ, 540, 113

Blanton, M. R., Eisenstein, D., Hogg, D. W., Schlegel, D. J., & Brinkmann, J. 2005a, ApJ, 629, 143

Blanton, M. R. & Roweis, S. 2007, AJ, 133, 734

Blanton, M. R., Schlegel, D. J., Strauss, M. A., Brinkmann, J., Finkbeiner, D., Fukugita, M., Gunn, J. E., Hogg, D. W., Ivezić, Ž., Knapp, G. R., Lupton, R. H., Munn, J. A., Schneider, D. P., Tegmark, M., & Zehavi, I. 2005b, AJ, 129, 2562

Boylan-Kolchin, M., Ma, C.-P., & Quataert, E. 2008, MNRAS, 383, 93

Brough, S., Forbes, D. A., Kilborn, V. A., & Couch, W. 2006, MNRAS, 370, 1223

Cameron, E. 2011, PASA, 28, 128

Carlberg, R. G., Yee, H. K. C., Ellingson, E., Morris, S. L., Abraham, R., Gravel, P., Pritchet, C. J., Smecker-Hane, T., Hartwick, F. D. A., Hesser, J. E., Hutchings, J. B., & Oke, J. B. 1997, ApJ, 485, L13

Chabrier, G. 2003, PASP, 115, 763

Chandrasekhar, S. 1943, ApJ, 97, 255

Conroy, C., Ho, S., & White, M. 2007, MNRAS, 379, 1491

De Lucia, G., Weinmann, S., Poggianti, B. M., Aragón-Salamanca, A., & Zaritsky, D. 2012, MNRAS, 423, 1277

Eke, V. R., Baugh, C. M., Cole, S., Frenk, C. S., King, H. M., & Peacock, J. A. 2005, MNRAS, 362, 1233

Gan, J.-L., Kang, X., Hou, J.-L., & Chang, R.-X. 2010, Research in Astronomy and Astrophysics, 10, 1242

Geller, M. J. & Huchra, J. P. 1983, ApJS, 52, 61

Hogg, D. W., Blanton, M. R., Brinchmann, J., Eisenstein, D. J., Schlegel, D. J., Gunn, J. E., McKay, T. A., Rix, H.-W., Bahcall, N. A., Brinkmann, J., & Meiksin, A. 2004, ApJ, 601, L29

Hou, A., Parker, L. C., & Harris, W. E. 2014, MNRAS, 442, 406

Jiang, C. Y., Jing, Y. P., Faltenbacher, A., Lin, W. P., & Li, C. 2008, ApJ, 675, 1095

McGee, S. L., Balogh, M. L., Bower, R. G., Font, A. S., & McCarthy, I. G. 2009, MNRAS, 400, 937

Oemler, Jr., A. 1974, ApJ, 194, 1

Poggianti, B. M., Desai, V., Finn, R., Bamford, S., De Lucia, G., Varela, J., Aragón-Salamanca, A., Halliday, C., Noll, S., Saglia, R., Zaritsky, D., Best, P., Clowe, D., Milvang-Jensen, B., Jablonka, P., Pelló, R., Rudnick, G., Simard, L., von der Linden, A., & White, S. 2008, ApJ, 684, 888

Pracy, M. B., Driver, S. P., De Propris, R., Couch, W. J., & Nulsen, P. E. J. 2005, MNRAS, 364, 1147

Presotto, V., Iovino, A., Scodeggio, M., Cucciati, O., Knobel, C., Bolzonella, M., Oesch, P., Finoguenov, A., Tanaka, M., Kovač, K., Peng, Y., Zamorani, G., Bardelli, S., Pozzetti, L., Kampczyk, P., López-Sanjuan, C., Vergani, D., Zucca, E., Tasca, L. A. M., Carollo, C. M., Contini, T., Kneib, J.-P., Le Fèvre, O., Lilly, S., Mainieri, V., Renzini, A., Bongiorno, A., Caputi, K., de la Torre, S., de Ravel, L., Franzetti, P., Garilli, B., Lamareille, F., Le Borgne, J.-F., Le Brun, V., Maier, C., Mignoli, M., Pellò, R., Perez-Montero, E., Ricciardelli, E., Silverman, J. D., Tresse, L., Barnes, L., Bordoloi, R., Cappi, A., Cimatti, A., Coppa, G., Koekemoer, A. M., McCracken, H. J., Moresco, M., Nair, P., & Welikala, N. 2012, A&A, 539, A55

Simard, L., Mendel, J. T., Patton, D. R., Ellison, S. L., & McConnachie, A. W. 2011, ApJS, 196, 11

Springel, V., White, S. D. M., Jenkins, A., Frenk, C. S., Yoshida, N., Gao, L., Navarro, J., Thacker, R., Croton, D., Helly, J., Peacock, J. A., Cole,

S., Thomas, P., Couchman, H., Evrard, A., Colberg, J., & Pearce, F. 2005, Nature, 435, 629

Taffoni, G., Mayer, L., Colpi, M., & Governato, F. 2003, MNRAS, 341, 434

Tal, T., Dekel, A., Oesch, P., Muzzin, A., Brammer, G. B., van Dokkum, P. G., Franx, M., Illingworth, G. D., Leja, J., Magee, D., Marchesini, D., Momcheva, I., Nelson, E. J., Patel, S. G., Quadri, R. F., Rix, H.-W., Skelton, R. E., Wake, D. A., & Whitaker, K. E. 2014, ApJ, 789, 164

van den Bosch, F. C., Pasquali, A., Yang, X., Mo, H. J., Weinmann, S., McIntosh, D. H., & Aquino, D. 2008, ArXiv e-prints

von der Linden, A., Wild, V., Kauffmann, G., White, S. D. M., & Weinmann, S. 2010, MNRAS, 404, 1231

Vulcani, B., De Lucia, G., Poggianti, B. M., Bundy, K., More, S., & Calvi, R. 2014, ApJ, 788, 57

Vulcani, B., Poggianti, B. M., Oemler, A., Dressler, A., Aragón-Salamanca, A., De Lucia, G., Moretti, A., Gladders, M., Abramson, L., & Halliday, C. 2013, A&A, 550, A58

Wetzel, A. R., Tinker, J. L., & Conroy, C. 2012, MNRAS, 424, 232

Wetzel, A. R., Tinker, J. L., Conroy, C., & van den Bosch, F. C. 2013, MNRAS, 432, 336

Yang, X., Mo, H. J., van den Bosch, F. C., & Jing, Y. P. 2005, MNRAS, 356, 1293

Yang, X., Mo, H. J., van den Bosch, F. C., Pasquali, A., Li, C., & Barden, M. 2007, ApJ, 671, 153

Zabludoff, A. I. & Mulchaey, J. S. 1998, ApJ, 496, 39

Ziparo, F., Popesso, P., Biviano, A., Finoguenov, A., Wuyts, S., Wilman, D., Salvato, M., Tanaka, M., Ilbert, O., Nandra, K., Lutz, D., Elbaz, D., Dickinson, M., Altieri, B., Aussel, H., Berta, S., Cimatti, A., Fadda, D., Genzel, R., Le Flo'ch, E., Magnelli, B., Nordon, R., Poglitsch, A., Pozzi, F., Portal, M. S., Tacconi, L., Bauer, F. E., Brandt, W. N., Cappelluti, N., Cooper, M. C., & Mulchaey, J. S. 2013, MNRAS, 434, 3089

This page intentionally left blank.